Cluster-Seeded Synthesis of Doped CdSe:Cu_4 Quantum Dots

Ali M. Jawaid,[†] Soma Chattopadhyay,[‡] Donald J. Wink,[†] Leah E. Page,[†] and Preston T. Snee[†,*]

[†]Department of Chemistry, University of Illinois at Chicago, 845 W. Taylor Street, Chicago, Illinois 60607-7061, United States, [‡]CSRRI-IIT, MRCAT, Argonne, National Laboratory, Sector 10, Building 433B, Argonne, Illinois 60439, United States, and Physics Department, Illinois Institute of Technology, Chicago, Illinois 60616, United States

ABSTRACT We report here a method for synthesizing CdSe quantum dots (QDs) containing copper such that each QD is doped with four copper ions. The synthesis is a derivative of the cluster-seed method, whereby organometallic clusters act as nucleation centers for quantum dots. The method is tolerant of the chemical identity of the seed; as such, we have doped four copper ions into CdSe QDs using $[Na(H_2O)_3]_2[Cu_4(SPh)_6]$ as a cluster seed. The controlled doping allows us to monitor the photophysical properties of guest ions with X-ray spectroscopy, specifically XANES and EXAFS at the copper K-edge. These data reveal that copper can capture both electrons and holes from photoexcited CdSe QDs. When the dopant is oxidized, photoluminescence is quenched and the copper ions translocate within the CdSe matrix, which slows the return to an emissive state.

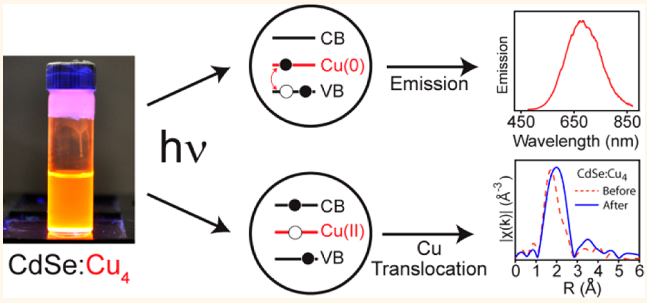

KEYWORDS: nanocrystals · quantum dots · cadmium selenide nanocrystals · doping · copper

Nanometer-sized semiconductor crystallites, or quantum dots (QDs), have garnered much attention due to their size-dependent optical and electronic properties.[1−5] Discrete size-dependent energy levels arise as the crystallite's boundaries become smaller than the Bohr exciton radius, a phenomenon known as quantum confinement. By modulating the size of the particle, it is possible to engineer the optical properties of these materials. Another method to tune quantum dot magneto-optical properties is to add guest impurities into the crystal lattice (*i.e.*, doping).[6−12] Presently, doped QDs can be prepared by a variety of methods, such as adding guests as organometallic precursors in the well-established rapid injection process.[4] Alternatively, dopants and semiconductor precursors, in the form of inorganic molecular clusters, can be added to a solvent and heated to spontaneously generate nuclei that grow into QDs.[8] Doping may also be achieved *via* cation exchange in as-prepared QDs.[13] These works have demonstrated that incorporating guest ions into a QD lattice can be very challenging. Temperature must be controlled to prevent self-annealing; furthermore, doping of the surface may simply result in fluorescence quenching.[11] Even when successful, the population of doped QDs has a Poissonian distribution of guest ions per QD. As recently demonstrated by Mocatta *et al.*,[13] QDs with different dopant levels have different properties (band gaps *etc.*); furthermore, the photophysical properties of the dopants themselves vary with respect to their concentration within the matrix.[8] As such, present methods to successfully introduce guest ions generate materials composed of individual QDs whose properties vary due to the Poissonian distribution of dopants per QD.

We present here a solution that produces doped QDs where every nanocrystal contains the same number of guest ions. The synthesis is based on the cluster-seed method developed by Pickett,[14,15] in which a known quantity of small organometallic clusters is added to a coordinating solvent with additional semiconductor precursors. Next, the temperature of the system is slowly increased, allowing for the clusters to function as QD nucleation sites, resulting in the formation of the same number of QDs as seeds; see Scheme 1. We found that the method is tolerant of the identity of the

* Address correspondence to sneep@uic.edu.

Received for review December 10, 2012 and accepted February 27, 2013.

Published online February 27, 2013
10.1021/nn305697q

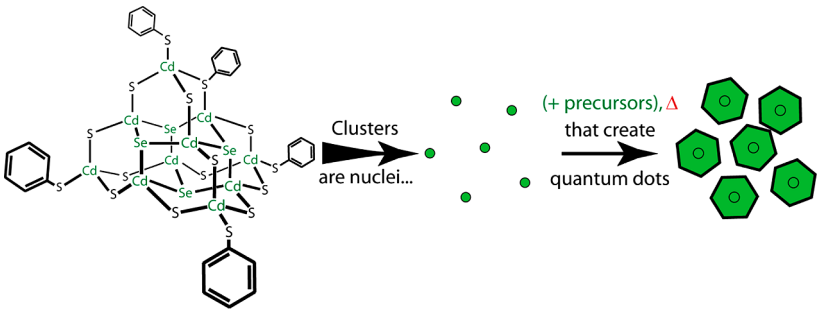

Scheme 1. Cluster-seed method for synthesizing quantum dots. The organometallic clusters act as nucleation points for the synthesis of the same number of QDs. Replacing $[NMe_4]_3Cd_{10}Se_4(SPh)_{16}$ for $[Na(H_2O)_3]_2[Cu_4(SPh)_6]$ clusters affords the formation of CdSe nanocrystals with four copper dopants.

cluster seed; as such, we used $[Na(H_2O)_3]_2[Cu_4(SPh)_6]$ clusters to seed the growth of CdSe QDs. All characterizations are consistent with the fact that each QD in our samples is doped with copper. Furthermore, we can demonstrate that exactly doping the sample is necessary to develop a fundamental understanding of the dopant photophysics.

RESULTS AND DISCUSSION

Cluster-Seed Method. Although the cluster-seed method of synthesizing quantum dots is known and even appears on Wikipedia,[14,15] we have not found a peer-reviewed report on the cluster-seed approach. As such, we examined the synthesis of CdSe QDs using $(NMe_4)_4[Cd_{10}Se_4(SPh)_{16}]$ clusters,[16] for which the method was designed.[14,15] In brief, a quantity of these clusters was added to 7 mL of octadecene and 1 mL of oleylamine with various cadmium and selenium precursors (generally cadmium acetylacetonate and diphenylphosphine selenide or tri-*n*-octylphosphine selenide). The solution was stirred at 50 °C for 24 h while the progress of the reaction was monitored continuously. After this time, the CdSe QDs were cooled and stored for later analysis. Detailed syntheses are described in the Methods section.

The presence of cluster seeds has profound effects on the nanocrystals synthesized. The number of QDs produced per batch was calculated as described in the Methods section.[17] The results, shown in Figure 1, demonstrate that the number of QDs produced in a typical synthesis is within 10% of the amount of seeds used. It is also noteworthy that the number of QDs produced with this method is ~20× greater than typically produced by the rapid injection procedure using the same amount of precursors. It was also found that CdSe QDs made with trioctylphosphine selenide have poor size distributions; however, the use of highly reactive diphenylphosphine selenide improves the monodispersity of the QDs, as evident by the sharp spectroscopic features seen in the absorption spectrum of the products (Figure1 inset). As a control, we also repeated the synthesis of QDs without seeds and found that only ~1.8 nm diameter[18] "magic-size"

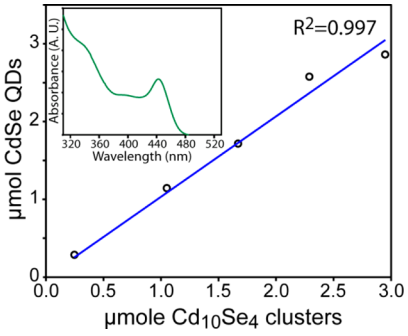

Figure 1. Regression of the number of moles of $(NMe_4)_4[Cd_{10}Se_4(SPh)_{16}]$ clusters *vs* the number of moles of quantum dots synthesized as calculated from ref 17. Inset shows the absorption spectrum of a sample prepared using diphenylphosphine selenide.

($Cd_{33}Se_{33}$) clusters are observed, as shown in Figure S1 of the Supporting Information.

The concentration of cluster seeds is a very important parameter. Within the linear range shown in Figure 1, increasing the concentration of seeds decreases the size of the QDs, as shown in Figure S2. This is the result of competition among an increasing number of QD nuclei (created by the presence of a larger number of seed clusters) for a finite number of precursors. We observe a break from the linearity shown in Figure 1 when using quantities of seeds outside of this range. In the nonlinear regimes, using a small cluster concentration resulted in the apparent formation of more CdSe QDs than clusters added. As "magic-size" clusters form when no seeds are present, we believe that $Cd_{33}Se_{33}$ clusters are also forming at very low seed concentrations, the absorption of which would create an apparent increase in the number of QDs. At high cluster concentrations, the calculated yield of nanoparticles was consistently lower than the number of cluster seeds. This is likely due to the fact that very small QDs should be produced that are not stable and undergo Ostwald ripening[19] or fuse to minimize surface energy.

These results demonstrate that the cluster-seed method can be used to control the number of QDs in a batch process. As it was originally intended, the

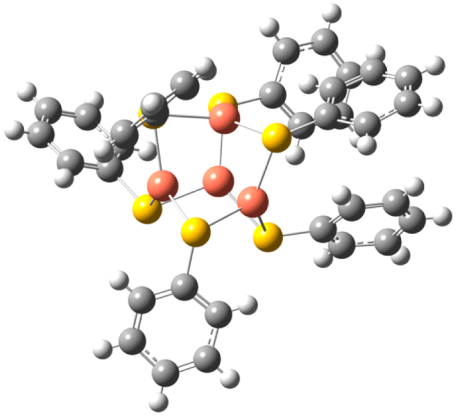

Figure 2. X-ray structure of $[Na(H_2O)_3]_2[Cu_4(SPh)_6]$; sodium ions and water have been removed for clarity. Orange: Cu(I), yellow: S, gray: C, white: H.

method allows for very large amounts of QDs to be synthesized at once; although, under the conditions employed, the QDs tend to be small and have a wider size distribution than that observed with the rapid injection procedure. We next sought to determine whether the growth of nanocrystals could be seeded using an organometallic cluster with a different elemental composition, as this would naturally lead to a method for doping QDs with a controlled number of ions.

Copper-Doped CdSe QDs. We chose to examine introducing copper guests into CdSe QDs for the first test on controlled doping. Doping copper ions into a CdSe QD is very difficult due to the small element's ability to diffuse through a semiconductor matrix.[11] Using a low-temperature synthetic method, such as that of Meulenberg *et al.*,[8] is necessary as a result. We have found the method of Meulenberg *et al.* to be highly reproducible; their reported process uses $(NMe_4)_2[Cu_4(SPh)_6]$ as a copper source and $(NMe_4)_4[Cd_{10}Se_4(SPh)_{16}]$ as a single-source precursor for cadmium and selenium. Heating these precursors to moderate temperatures created Cu-doped CdSe QDs; however, as the clusters are also precursors, the dopant levels must follow Poisson statistics. We have synthesized several samples of such Poissonian doped CdSe:Cu$_{\leftrightarrow}$ QDs to compare their properties to our materials. We thought to use the same copper cluster as a seed in our studies given the success of the method developed by Meulenberg *et al.* However, when synthesizing $(NMe_4)_2[Cu_4(SPh)_6]$ using a previously published protocol,[16] clusters with multiple nuclearities are produced, such as $Cu_5(SPh)_7^{2-}$ and $Cu_6(SPh)_8^{2-}$ and additional uncharacterized products.[20] To circumvent this issue, the synthesis was re-engineered to produce a single product, $[Na(H_2O)_3]_2[Cu_4(SPh)_6]$ (Cu_4 clusters), as determined from the crystal structure shown in Figure 2. When used as nuclei in the cluster-seed method, zinc blende (Figure S3) CdSe nanocrystal growth occurs rapidly and absorption profiles (Figure S4) are similar to

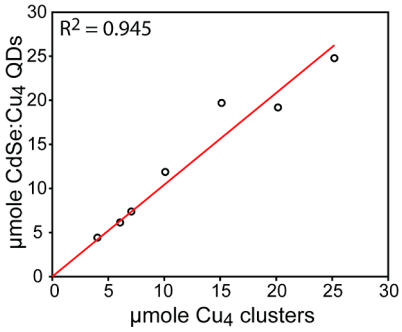

Figure 3. Regression of the number of moles of $[Na(H_2O)_3]_2[Cu_4(SPh)_6]$ clusters *vs* the number of moles of quantum dots synthesized as calculated from ref 17. Removing the anomalous point at ~15 μmol of Cu_4 clusters results in a fit with an R^2 of 0.994.

those of undoped samples. A linear plot is obtained when comparing the moles of Cu_4 clusters to the moles of QDs synthesized, as shown in Figure 3, which is highly indicative of copper clusters acting as nucleation points for CdSe:Cu_4 QDs.

The absorption spectra of doped nanocrystals oddly indicate that the use of more Cu_4 clusters during QD syntheses resulted in the formation of larger nanocrystals with smaller band gaps; as such, two of the larger samples were characterized with TEM microscopic analysis. The data shown in Figure S5 indicate that the use of more clusters creates smaller quantum dots, the same phenomenon observed in the synthesis of pure CdSe QDs. However, the effect of doping increases the apparent band gaps such that the sizes of the nanocrystals are larger than expected based on the absorption onsets. These odd observations may be explained by a size-dependence on the effect of band-gap alteration with doping, where the increase of the band gap is mitigated, or even perhaps reversed, when doping smaller QDs. In fact, such complex size-dependent alterations of QD band gaps due to doping were predicted by Moccata *et al.* for Cu-doped InAs nanocrystals.[13]

Samples were tested using several methods to confirm copper doping. The emission of CdSe:Cu_4 QDs was compared with Poissonian copper-doped CdSe:Cu$_{\leftrightarrow}$ nanocrystals synthesized by the method of Meulenberg *et al.*;[8] both samples were found to have similar emissive dopant signatures, as shown in Figure 4. However, band-edge emission is observed from the Poisson doped samples that must be due to the fact that some nanocrystals have little to no dopants. This is not true for a significant majority of exactly doped CdSe:Cu_4 samples where no QD band-edge emission is observed, despite the fact that the Poissonian copper-doped quantum dots contain 8× more copper than our samples, as discussed below. XPS analysis of CdSe:Cu_4 QDs shows a peak consistent with excitation of a Cu 2p electron, although the feature is very weak (Figure S7), as expected given the low level of copper

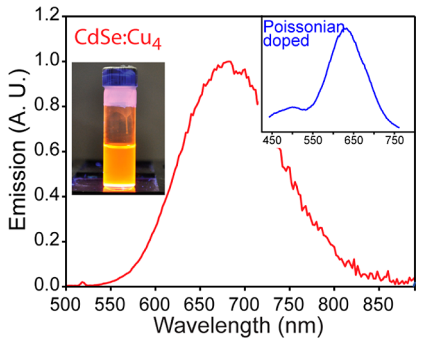

Figure 4. $CdSe:Cu_4$ QD emission spectrum displays no evidence of core QD emission. The small peak at 518 nm is due to a Raman transition of the solvent. Inset: Emission spectrum from Poissonian doped $CdSe:Cu_{\sim}$ QDs displays some core QD emission at ~500 nm, likely from undoped nanocrystals.

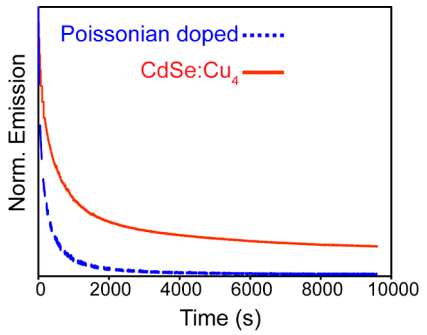

Figure 5. Cu emission from all copper-doped quantum dots is quickly and severely photodarkened.

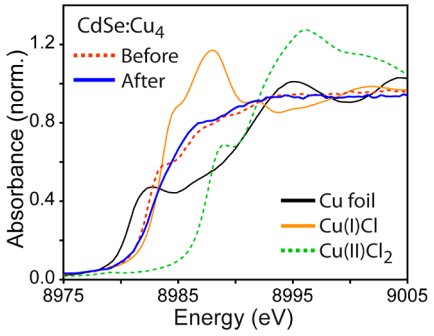

Figure 6. Cu K-edge XANES spectra of copper foil, $Cu(II)Cl_2$, and Cu(I)Cl demonstrate that $CdSe:Cu_4$ QDs (red dashed line, "before") are in the +1 oxidation state. The X-ray absorption onset moves to a higher energy after photodarkening the sample (blue line, "after"); this is indicative of copper oxidation.

doped in the CdSe QDs. Tests were performed to verify that the copper dopants were incorporated into the CdSe lattice and not on the QD surface; these data are shown in Figure S6 of the Supporting Information. In these studies, dopant-centered emission was observed before and after cleaning the surface with pyridine,[6] although the overall quantum yield was lowered likely due to exciton trapping to defective surface states.

Elemental analysis on processed $CdSe:Cu_4$ samples provides evidence that the cluster-seed method exactly dopes quantum dots; the results are summarized in Table S1. All QDs were rigorously processed by multiple precipitations to remove unreacted copper and then digested in acid for analysis with flame atomic absorption. The amount of copper found in the $CdSe:Cu_4$ QD sample was somewhat less than expected (~67%); we attribute the loss of some copper due to the processing before digestion. In comparison, Poissonian doped $CdSe:Cu_{\sim}$ samples retain only ~22% of the copper used in the synthesis. Furthermore, it should be noted that 8× less copper was used in the synthesis of $CdSe:Cu_4$ compared to $CdSe:Cu_{\sim}$ QD yet incorporated 3× more of the available copper into the CdSe matrix while simultaneously synthesizing 10× more quantum dots. There is no evidence of excess copper in the solvent after precipitation of $CdSe:Cu_4$QDs that can react with other precursors to form dark-colored precipitates,[12] which is often seen in $CdSe:Cu_{\sim}$ supernatants. Overall, the sum of these studies is highly indicative that the cluster-seed method is tolerant of the use of seeds that do not contain the same elemental composition as the QD matrix, leading, in this example, to a robust method for synthesizing CdSe QDs with exactly four copper ion guests.

Light-Induced Dopant Reduction. We have found that it is necessary to control dopant stoichiometry to properly characterize some aspects of dopant photophysics. In the present study, significant photodarkening of the emission from $CdSe:Cu_4$ and Poissonian copper-doped CdSe QDs was observed when exposed to prolonged irradiation, as shown in Figure 5. The kinetics of the photodarkening is multiexponential; additionally, we noticed that the photodarkening of the Cu-doped nanocrystals is slowly reversible over the course of hours. We hypothesized that the severe photodarkening is due to a redox process, most likely a Cu^+ to Cu^{2+} transition. The oxidation may result in a physical transformation that is facilitated by copper's ability to diffuse within a crystal lattice,[11] making a return to the emissive state a slow process.

Cu K-edge XANES and EXAFS spectroscopy were used to test this model and to determine the nature of the observed decay dynamic; these experiments were performed using the Advanced Photon Source at Argonne National Laboratory. XANES can characterize the oxidation state of the Cu before and after photoirradiation, and EXAFS spectroscopy can determine the nearest neighbor scattering profiles of Cu. This was used to characterize the local environment of copper dopants before and after prolonged UV irradiation in exactly doped $CdSe:Cu_4$ QDs. When the sample is in the emissive state, XANES spectroscopy of $CdSe:Cu_4$ shows a Cu K-edge at ~8980 eV (Figure 6), which aligns well with Cu^+ standards including the Cu_4 clusters used in the synthesis of these materials. Samples were then irradiated at 365 nm until the emission was fully

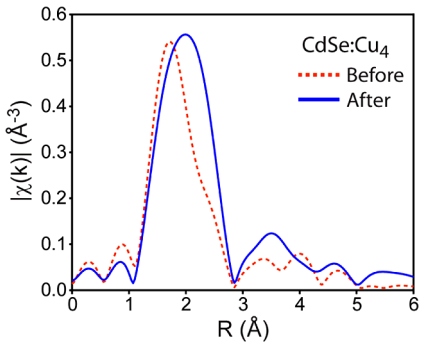

Figure 7. EXAFS scattering radial distribution of CdSe:Cu_4 QDs (red dash line) shifts to longer distances after photodarkening (blue solid line) due to copper dopants translocating within the quantum dot matrix as evident from fits to the data.

quenched, at which time the X-ray absorption spectrum was remeasured. As shown in Figure 6, the Cu K-edge of CdSe:Cu_4 QDs slightly shifts to a higher energy, indicating that the copper dopants are oxidized. EXAFS data of the same sample before and after photodarkening (Figure 7) show that the nearest neighbor scattering amplitude has shifted to a longer distance. Fitting the EXAFS data reveals that Cu electrons are scattering from sulfur and selenium centers, which indicates that the original cluster seeds are partially intact in the QDs. After photodarkening, however, electrons are predominantly scattering off selenium, as shown in Table S2 of the Supporting Information. While this could be due to changes in the structure of the nearest coordination sphere of the dopants, it is more likely that the redox-active copper ions are translocating within the nanocrystal matrix as a result of oxidation by the photogenerated exciton. Overall, the oxidation of copper suppresses the dopant emission *via* translocation and must result in an exciton trap state for radiative excitonic recombination, as no band-edge emission is observed. The translocation of the dopant hinders, but does not fully suppress, a transformation back to the original +1 oxidation state, as evidenced by the very long time scale of fluorescence recovery after UV irradiation.

This observation helps answer a long-standing question concerning the nature of copper-dopant-centered emission, which is dependent on the size of the nanocrystal host. Presently, the standard model is that a single photogenerated QD exciton charge carrier is trapped by the guest ion and later recombines with the other charge carrier located in a QD band. Thus, the size dependence of the QD electronic structure is still evident in the guest ion emission. Our present investigation and a previous study have concluded that emission results from copper-trapped electrons recombining with QD valence holes in Cu-doped CdSe nanocrystals.[8] However, reports on Cu-doped ZnS,[12] ZnSe,[21−24] and InP[25] nanocrystals have demonstrated the exact opposite based upon trends in the dopant

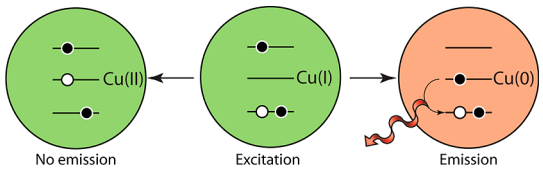

Scheme 2. Emission and photodarkening most likely results from separate redox properties. Emission originates from Cu-bound electrons recombining with QD valence holes, while photodarkening is the result of dopant oxidation.

emission wavelength as a function of the semiconductor host electronic structure and the influence of magnetic fields on dopant photophysics. As such, it appears there is no consensus on the origin of Cu-dopant emission from within nanocrystal matrices; however, note that the question of whether copper is either an exciton electron or a hole trap is very black and white. Our data demonstrate that copper dopants can act as either electron or hole traps simultaneously (Scheme 2). Thus, conflicting results from studies performed in different semiconductor hosts are likely due to biasing the photochemical dynamics toward a particular route most likely due to subtleties in the host electronic structure.

A natural question to ask is whether the use of exactly doped QDs is necessary to observe the photophysics reported. Shown in Figures S8 and S10 of the Supporting Information are the XANES and EXAFS spectra of Poissonian doped CdSe:$Cu_{\leftrightarrow}$ QDs before and after photodarkening. The XANES Cu K-edge data reveal that dopants are in the +1 oxidation state, which is entirely consistent with the previous report on X-ray L-edge spectroscopy of Poissonian doped CdSe:$Cu_{\leftrightarrow}$ QDs.[8] The oxidation of the dopants upon photodarkening the sample is also evident; however, only minor differences are noted in the EXAFS scattering profiles before and after photodarkening, as sulfur nearest neighbors are seen in both data sets. We attribute this to the varying nature of dopant concentration as dictated by Poisson statistics, especially as the majority of dopants reside in individual QDs with higher dopant levels. The excess unoxidized dopants likely overwhelm the EXAFS spectrum such that the translocation of a minority of oxidized copper guests is not observed.

CONCLUSION

We have demonstrated a method for producing doped quantum dots by a modification of the cluster-seed method to avoid the issues associated with characterizing Poissonian doped samples. The correlation of moles of clusters to QDs produced in a batch, the lack of core emission, and XPS and elemental analysis are all consistent with the synthesis of CdSe:Cu_4 QDs. The observation of photodarkening was unexpected; however, we have been able to describe the fundamental photophysics and unravel interesting

dynamics of the dopants as a function of photoexcitation. Some aspects of dopant dynamics require the use of exactly doped QD systems. The fact that the method appears insensitive to the elemental composition of the organometallic seed offers the opportunity to study a very wide array of doped QD systems.

METHODS

Materials. 1-Octadecene (90%), oleylamine (90%), benzenethiol (97%), pyridine (98%), anhydrous methanol (99.8%), triethylamine (97%), acetonitrile (99.9%), toluene (99.9%), cadmium acetylacetonate (99.999%), triphenylphosphine (99%), and tetramethylammonium chloride (99%) were purchased from Sigma-Aldrich. Anhydrous dimethylformamide (DMF, 99.8%) and copper(II) nitrate trihydrate (99%) was purchased from Acros. Cadmium nitrate tetrahydrate (99.99%) trioctylphosphine (97%), selenium shot (99.999%), and selenium powder (99.999%) were purchased from Strem. Lithium wire (>99.5%) and copper traceable standard (998 ± 4 mg/L) for atomic absorption spectroscopy were purchased from Fluka. 1-Octadecene and oleylamine were distilled and stored in an MBraun inert atmosphere glovebox. Triphenylphosphine was recrystallized from boiling ethanol and stored under ambient conditions. A 1 M TOPSe solution was prepared by mixing selenium shot and trioctylphosphine in an inert atmosphere. All other reagents were used without further purification.

$(NMe_4)_2[Cd_4(SPh)_{10}]$ Synthesis. Into a one-neck round-bottom flask, 40 mL of methanol and 25 mL (180 mmol) of triethylamine were added. After 1 h of flushing with N_2, 20 mL (195 mmol) of benzenethiol was added to this solution. The solution became warm and was allowed to cool to room temperature. Next, 21.0 g (89 mmol) of $Cd(NO_3)_2 \cdot 3H_2O$ dissolved in 40 mL of methanol was quickly added to the solution, which became slightly cloudy during the addition of the last few milliliters of $Cd(NO_3)_2$. Finally, 8.00 g (73 mmol) of tetramethylammonium chloride was added. The solution turned clear (within 5 min), and the solution was allowed to stand without stirring. Precipitation of crystals occurred over the course of 12 h and sometimes required cooling to induce crystallization. The clusters were washed thoroughly with methanol and ethanol, dried, and recrystallized from acetonitrile by addition of toluene at room temperature.

$(NMe_4)_4[Cd_{10}Se_4(SPh)_{16}]$ Synthesis. Into a one-neck round-bottom flask, 1.0 g (0.55 mmol) of $(NMe_4)_2[Cd_4(SPh)_{10}]$ was added and dissolved with 2.0 mL of acetonitrile. In one portion, 44 mg of Se (0.56 mmol) was added under N_2 flow. The black heterogeneous solution slowly turned white, which indicated the reaction was complete. After no selenium particles were visible, the vessel was heated to 80 °C and acetonitrile was slowly added until all the precipitate had dissolved. The solution had a slight yellow tint. After all precipitate had dissolved, the solution was allowed to cool to room temperature. The product crystallized out of solution over the course of 8 h. The crystals were collected, washed with acetonitrile, and dried. Recrystallization can be afforded from DMF with addition of diethyl ether.

$[Na(H_2O)_3]_2[Cu_4(SPh)_6]$ Synthesis. Into a one-neck round-bottom flask equipped with a dripping funnel, 50 mL of methanol, 25 mL of triethylamine, and 10 g of benezenethiol (97 mmol) were added, and the solution was then flushed with N_2 for 1 h. The solution was then heated to reflux, upon which 2.20 g (9.2 mmol) of $Cu(NO_3)_2 \cdot 3H_2O$ dissolved in 40 mL of methanol was added dropwise. The solution quickly turned yellow and remained a yellow color throughout the process. Addition of the copper nitrate solution was stopped when the reaction vessel was saturated with product, evaluated by the increasingly lower solubility of $Cu(NO_3)_2$. If too much $Cu(NO_3)_2$ is added, amorphous yellow $Ph_2S_2Cu_2$ solids precipitate out immediately. After the solution cooled to room temperature, 1.36 g (23 mmol) of NaCl dissolved in methanol was added to the solution, which was layered with 2-propanol immediately, and allowed to equilibrate at room temperature under N_2 overnight. The product crystallized as yellow crystals, which were filtered, washed with cold acetone and ether, dried under vacuum, and stored under N_2 in a glovebox. The clusters are soluble in DMF and acetonitrile and stable for hours in both solutions; however, they do decompose slowly, which can be monitored by the emergence of a red fluorescence associated with the formation of $Ph_2S_2Cu_2$. This decomposition product also impedes recrystallization from acetonitrile or DMF. Storage of these clusters at ambient conditions results in oxidation to $Ph_2S_2Cu_2$, a pastel yellow byproduct. The supernatant contains additional products that can be isolated by addition of water. These colorless crystals have not been characterized. They do, however, decompose to $Ph_2S_2Cu_2$ if left in the reaction solution or exposed to ambient conditions.

Diphenylphosphine Synthesis. Into a three-neck round-bottom flask equipped with a condenser and dripping funnel, triphenylphosphine (5.00 g) and Li wire (0.70 g) were added, and the solution was dried under vacuum for 1 h and backfilled with N_2. THF (50 mL) was dripped in under a vigorous stir. The solution turned a deep red color and heat was evolved. The solution was allowed to stir for 3 h and cooled to room temperature, indicating the reaction was complete. The solution was filtered through glass wool and then cooled on ice. H_2O was added to liberate the diphenylphosphinium salt, and after addition of ~5 mL of ether the solution was washed with brine. The organic layer was dried under Na_2SO_4, and the solvent was removed under vacuum, leaving a clear oil, which was distilled with heat under vacuum (bp 157 °C at 200 mTorr, 3.1 g, 57% yield) and stored under N_2.

Diphenylphosphine Selenide (DPPSe) Synthesis. Into a one-neck round-bottom flask equipped with a condenser, diphenylphosphine (3.1 g), toluene (20 mL), and selenium shot (1 equiv, 1.32 g) were added, and the mixture was slowly heated to a gentle reflux overnight. The solution turned clear during the reaction. The solvent was removed through rotary evaporation and stored under N_2. Recrystallization can be afforded through addition of a minimum amount of toluene and heated to just under reflux. Crystals appear after slowly cooling to room temperature and leaving still overnight at 4 °C.

CdSe Synthesis Using $(NMe_4)_4[Cd_{10}Se_4(SPh)_{16}]$. Into a three-neck flask was added 7 mL of octadecene, 1 mL of oleylamine, and 0.264 g (1 mmol) of $Cd(C_5H_8O_2)_2$, and the solution was heated to 110 °C under vacuum for 1 h. The solution turned clear, and after the pressure stabilized, the vessel was backfilled with N_2 and cooled to room temperature. At room temperature, 0.5−56 mg of $(NMe_4)_4[Cd_{10}Se_4(SPh)_{16}]$ was added (0.15−16.75 μmol), and 5 mL of a 1 M TOPSe solution was slowly added (0.1 mL/min). Experiments with DPPSe used 0.5 mmol of the precursor dissolved in a minimal amount of toluene (~0.5 mL); this solution was added dropwise at room temperature. After addition of the selenium precursor was complete, the vessel was slowly heated to 50 °C for 24 h. A control experiment was performed exactly as above without the addition of $(NMe_4)_4[Cd_{10}Se_4(SPh)_{16}]$ clusters using TOPSe. All samples were purified by precipitation with hexane/ethanol and subsequent redispersion into hexane, whereupon a known mass of a sample was extracted and the optical absorption spectrum was measured. The empirical formula derived by Peng *et al.*[17] was used to determine the absorption cross section and thus QD concentration. These data were plotted as a function of the number of cluster seeds used in the synthesis as shown in Figure 1.

CdSe:Cu_4 Synthesis Using $[Na(H_2O)_3]_2[Cu_4(SPh)_6]$. Into a three-neck flask were added 7 mL of octadecene, 1 mL of oleylamine, and 0.264 g (1 mmol) of $Cd(C_5H_8O_2)_2$ and was heated to 110 °C under vacuum for 1 h. The solution turned clear, and after the pressure stabilized, the vessel was backfilled with N_2 and cooled to room temperature. Next, 4−25 mg of $[Na(H_2O)_3]_2[Cu_4(SPh)_6]$ (4−25 μmol) was added in enough DMF to dissolve completely (~0.1 mL), and the solution was added at room temperature to the degassed solvent. Finally, 0.5 mmol of DPPSe in a minimal amount of toluene (~0.5 mL) was added dropwise at room temperature; the solution was then slowly heated to 50 °C and monitored *via* absorption. It should be noted that the use of

$[Na(H_2O)_3]_2[Cu_4(SPh)_6]$ clusters is incompatible with TOPSe, the use of which resulted in frequent precipitations, as evident by formation of a black precipitate or by dissolution of Cu^+ ions into solution. We also note that great care must be taken to ensure that the solvents have been properly degassed; otherwise the synthesis results predominately in the formation of black precipitates.

CdSe:Cu$_{\sim}$ Synthesis. Into a three-neck round-bottom flask, 0.040 g of $[Na(H_2O)_3]_2[Cu_4(SPh)_6]$ and 0.120 g of $(NMe_4)_4[Cd_{10}Se_4(SPh)_{16}]$ were added and dried under vacuum for 1 h and backfilled with N_2 gas. Hexadecylamine was dried at 100 °C in a separate vessel and added to the clusters, and the mixture was slowly heated to 250 °C (~5 °C/min) while monitoring for Cu emission. Nanocrystal growth can be observed at ~150 °C, and Cu emission can be seen at ~175 °C.

Pyridine Surface Cleaning. Doped CdSe:Cu_4 QDs were precipitated twice through the addition of ethanol and were redispersed in a minimal amount of toluene. Pyridine was added to this solution, and the solution was allowed to stir at 50 °C overnight and again precipitated twice from toluene. The nanocrystals were recapped with oleylamine. This process ensures that any possible surface-bound copper is removed, and the resulting nanocrystal suspension was analyzed using fluorescence spectroscopy. The absorption was observed to blue-shift by ~4 nm, indicating that the samples were etched, albeit minimally so.

Atomic absorption spectroscopy standards were prepared by a NIST-traceable solution. Nanocrystals were precipitated until they were no longer soluble in hexane. Digestion of nanocrystal samples was done under boiling HNO_3 (Cu < 0.05 ppm) in an acid-cleaned Teflon beaker. The samples were diluted using 10 MΩ H_2O.

Characterization. A UV−vis Biorad 300 Cary spectrophotometer was used for absorption measurements. Emission data were taken on a custom-made Horiba Jobin Yvon Fluorolog-3 spectrofluorometer with a short-arc xenon lamp at an excitation of 400 nm. Atomic absorption spectroscopy was performed using a PerkinElmer AAnalyst 200.

The single-crystal X-ray diffraction study of $[Na(H_2O)_3]_2[Cu_4(SPh)_6]$ was done on a deep yellow block with approximate dimensions 0.28 mm × 0.15 mm × 0.12 mm. The crystal was evaluated, and data were collected in air at ambient temperature. The crystal evaluation and data collection were performed on a Bruker AXS diffractometer with Mo Kα (λ = 0.71073 Å) radiation and an area detector. The final cell constants were calculated from reflections from the actual data collection. The data were collected by using the multiscan data collection routine. A total of 68 105 data were collected. Of these data, 12 043 unique reflections were available, with an R_{int} of 0.102. There were 6654 reflections with $I > 2\sigma(I)$. These were corrected for absorption using semiempirical methods (SADABS). Solution of the structure was accomplished in the hexagonal space group $P3_1c$ with $Z = 6$. Molecules of the $[Cu_4(SPh)_6]$ cluster were situated on 3-fold rotation and screw axes of the space group. Refinement of the data gave $wR_2 = 0.2183$ and $R = 0.1512$ for all data and $R = 0.0751$ for data with $I > 2\sigma(I)$.

EXAFS and XANES measurements at the Cu K-edge (8979 eV) were carried out at the MRCAT 10-ID beamline at the Advanced Photon Source at Argonne National Laboratory[26] to study the local environment of Cu dopants before and after photodarkening with UV light. Doped QD samples were dissolved in toluene and were loaded in 0.5 mL circular safe-lock plastic tubes from Eppendorf. The wall thickness of these circular cuvettes is 700 μm; the absorption of the walls at 8979 eV (Cu K-edge) is 0.392. Hence, the absorption of the walls is minimal and does not affect the data concerning the Cu-edge absorption energy. The samples were placed at a 45° orientation to the beam, and all measurements were performed at room temperature. X-ray absorption measurements were made in fluorescence mode using a four-element Vortex 411 solid-state fluorescence detector in step-scan mode. The step size across the edge was 0.25 eV, and the measurement time was set to 2 s per point. XANES scans covered −250 eV below copper's K-edge energy (8979 eV) up to 300 eV above the Cu edge. EXAFS scans on quantum dots were started −250 eV below the Cu edge up to 800 eV above. A typical scan took about 20 min with data in higher k-space taken with a step size of k = 0.05 Å^{-1} and measurement time of 4 s per step. The energy resolution of the monochromator is 0.25 eV. The position of the X-ray beam was moved between each scan to minimize sample degradation. EXAFS measurements were also performed in a transmission geometry to measure the X-ray absorption of $CuCl_2$, CuCl, CuO, Cu_2O, CuSe, and Cu_2Se powders to provide standards to determine the oxidation state of Cu in doped QD samples. Each reference was spread over kapton tape and subsequently stacked together such that the thickness (x) of the samples corresponded to $\Delta\mu x = 0.5$, where $\Delta\mu$ is the edge step of the absorption coefficient at the Cu K-edge energy. All standards were measured in a transmission geometry using a quick scan mode with the monochromator measuring energy on the fly. The scans of Cu standards used step sizes of 0.3 eV and a measurement time of 0.1 s per step. Several scans were taken on each standard and were subsequently merged for better statistics. A copper metal foil scan was simultaneously measured with every standard and QD sample using a reference ion chamber to calibrate the energy scale. These measurements used a reference detector composed of 70% He/30% N_2 and a transmission reference of 100% N_2. All measurements used an incident X-ray spot size of 500 × 500 μm.

All data were processed using the Athena software[27] by extracting the EXAFS oscillations $\chi(k)$ as a function of photoelectron wavenumber k following standard procedures. Theoretical models were generated using FEFF6[28] in the conventional way using the fitting program Artemis.[29] Fitting parameters were obtained by modeling the EXAFS data of each sample in R-space, with k-weights of 1, 2, and 3, until a satisfactory description of the system was obtained.

Conflict of Interest: The authors declare no competing financial interest.

Supporting Information Available: Additional characterization data, such as absorption and X-ray photoelectron spectrum of QDs, XANES and EXAFS of Poissonian doped CdSe:Cu$_{\sim}$ QDs, as well as elemental analysis results. This material is available free of charge *via* the Internet at http://pubs.acs.org.

Acknowledgment. We would like to thank Carlo Segre, Jeffery Miller, Tomohiro Shibata, Vladislav Zyryanov, and Shelly Kelly for assistance with X-ray absorption spectroscopy measurements made at Argonne National Laboratory as well as analyses of the data. We also thank Luke Hanley, Randall Meyer, and Michael Trenary of UIC for helpful discussions. Support for this research was provided by the UIC and the UIC Chancellor's Discovery Fund. Acknowledgment is made to the Donors of the American Chemical Society Petroleum Research Fund (50859-ND10) for partial support of this research. MRCAT operations are supported by the Department of Energy and the MRCAT member institutions. The use of the Advanced Photon Source at ANL was supported by the U.S. Department of Energy, Office of Science, Office of Basic Energy Sciences, under Contract No. DE-AC02-06CH11357.

REFERENCES AND NOTES

1. Rossetti, R.; Nakahara, S.; Brus, L. E. Quantum Size Effects in the Redox Potentials, Resonance Raman-Spectra, and Electronic-Spectra of CdS Crystallites in Aqueous-Solution. *J. Chem. Phys.* **1983**, *79*, 1086–1088.
2. Ekimov, A. I.; Onushchenko, A. A. Size Quantization of the Electron Energy Spectrum in a Microscopic Semiconductor Crystal. *JETP Lett.* **1984**, *40*, 1136–1139.
3. Bawendi, M. G.; Steigerwald, M. L.; Brus, L. E. The Quantum-Mechanics of Larger Semiconductor Clusters (Quantum Dots). *Annu. Rev. Phys. Chem.* **1990**, *41*, 477–496.
4. Murray, C. B.; Norris, D. J.; Bawendi, M. G. Synthesis and Characterization of Nearly Monodisperse CdE (E = S, Se, Te) Semiconductor Nanocrystallites. *J. Am. Chem. Soc.* **1993**, *115*, 8706–8715.
5. Alivisatos, A. P.; Harris, A. L.; Levinos, N. J.; Steigerwald, M. L.; Brus, L. E. Electronic States of Semiconductor Clusters - Homogeneous and Inhomogeneous Broadening of the Optical-Spectrum. *J. Chem. Phys.* **1988**, *89*, 4001–4011.

6. Norris, D. J.; Yao, N.; Charnock, F. T.; Kennedy, T. A. High-Quality Manganese-Doped ZnSe Nanocrystals. *Nano Lett.* **2001**, *1*, 3–7.
7. Erwin, S. C.; Zu, L. J.; Haftel, M. I.; Efros, A. L.; Kennedy, T. A.; Norris, D. J. Doping Semiconductor Nanocrystals. *Nature* **2005**, *436*, 91–94.
8. Meulenberg, R. W.; van Buuren, T.; Hanif, K. M.; Willey, T. M.; Strouse, G. F.; Terminello, L. J. Structure and Composition of Cu-Doped CdSe Nanocrystals Using Soft X-Ray Absorption Spectroscopy. *Nano Lett.* **2004**, *4*, 2277–2285.
9. Beaulac, R.; Schneider, L.; Archer, P. I.; Bacher, G.; Gamelin, D. R. Light-Induced Spontaneous Magnetization in Doped Colloidal Quantum Dots. *Science* **2009**, *325*, 973–976.
10. Chikan, V. Challenges and Prospects of Electronic Doping of Colloidal Quantum Dots: Case Study of CdSe. *J. Phys. Chem. Lett.* **2011**, *2*, 2783–2789.
11. Chen, D.; Viswanatha, R.; Ong, G. L.; Xie, R.; Balasubramaninan, M.; Peng, X. Temperature Dependence of "Elementary Processes" in Doping Semiconductor Nanocrystals. *J. Am. Chem. Soc.* **2009**, *131*, 9333–9339.
12. Srivastava, B. B.; Jana, S.; Pradhan, N. Doping Cu in Semiconductor Nanocrystals: Some Old and Some New Physical Insights. *J. Am. Chem. Soc.* **2011**, *133*, 1007–1015.
13. Mocatta, D.; Cohen, G.; Schattner, J.; Millo, O.; Rabani, E.; Banin, U. Heavily Doped Semiconductor Nanocrystal Quantum Dots. *Science* **2011**, *332*, 77–81.
14. Pickett, N. (Nanoco Technologies Limited, GB) Controlled Preparation of Nanoparticle Materials. U.S. Patent 7,867,556, October 27, 2006.
15. http://en.wikipedia.org/wiki/Quantum_dot.
16. Dance, I. G.; Choy, A.; Scudder, M. L. Synthesis, Properties, and Molecular and Crystal-Structures of $(Me_4N)_4[E_4M_{10}(SPh)_{16}]$ (E = S, Se; M = Zn, Cd): Molecular Supertetrahedral Fragements of the Cubic Metal Chalcogenide Lattice. *J. Am. Chem. Soc.* **1984**, *106*, 6285–6295.
17. Yu, W. W.; Qu, L. H.; Guo, W. Z.; Peng, X. G. Experimental Determination of the Extinction Coefficient of CdTe, CdSe, and CdS Nanocrystals. *Chem. Mater.* **2003**, *15*, 2854–2860.
18. Kilina, S.; Ivanov, S.; Tretiak, S. Effect of Surface Ligands on Optical and Electronic Spectra of Semiconductor Nanoclusters. *J. Am. Chem. Soc.* **2009**, *131*, 7717–7726.
19. Talapin, D. V.; Rogach, A. L.; Haase, M.; Weller, H. Evolution of an Ensemble of Nanoparticles in a Colloidal Solution: Theoretical Study. *J. Phys. Chem. B* **2001**, *105*, 12278–12285.
20. Dance, I. G.; Bowmaker, G. A.; Clark, G. R.; Seadon, J. K. The Formation and Crystal and Molecular Structures of Hexa-(μ-Organothiolato)Tetracuprate(I) Cage Dianions: Bis-(Tetramethylammonium)Hexa-(μ-Methanethiolato)Tetracuprate-(I) and 2 Polymorphs of Bis(Tetramethylammonium)Hexa-(μ-Benzenethiolato)-Tetracuprate(I). *Polyhedron* **1983**, *2*, 1031–1043.
21. Corrado, C.; Jiang, Y.; Oba, F.; Kozina, M.; Bridges, F.; Zhang, J. Z. Synthesis, Structural, and Optical Properties of Stable ZnS:Cu,Cl Nanocrystals. *J. Phys. Chem. A* **2009**, *113*, 3830–3839.
22. Pradhan, N.; Goorskey, D.; Thessing, J.; Peng, X. G. An Alternative of CdSe Nanocrystal Emitters: Pure and Tunable Impurity Emissions in ZnSe Nanocrystals. *J. Am. Chem. Soc.* **2005**, *127*, 17586–17587.
23. Viswanatha, R.; Brovelli, S.; Pandey, A.; Crooker, S. A.; Klimov, V. I. Copper-Doped Inverted Core/Shell Nanocrystals with "Permanent" Optically Active Holes. *Nano Lett.* **2011**, *11*, 4753–4758.
24. Suyver, J. F.; van der Beek, T.; Wuister, S. F.; Kelly, J. J.; Meijerink, A. Luminescence of Nanocrystalline ZnSe:Cu. *Appl. Phys. Lett.* **2001**, *79*, 4222–4224.
25. Xie, R.; Peng, X. Synthesis of Cu-Doped InP Nanocrystals (D-Dots) with ZnSe Diffusion Barrier As Efficient and Color-Tunable NIR Emitters. *J. Am. Chem. Soc.* **2009**, *131*, 10645–10651.
26. Segre, C. U.; Leyarovska, N. E.; Chapman, L. D.; Lavender, W. M.; Plag, P. W.; King, A. S.; Kropf, A. J.; Bunker, B. A.; Kemner, K. M.; Dutta, P.; Duran, R. S.; Kaduk, J. The MRCAT insertion device beamline at the Advanced Photon Source. *Synchrotron Radiation Instrumentation, AIP Conference Proceedings* **2000**, *521*, 419–422.
27. Newville, M. Ifeffit: Interactive XAFS Analysis and FEFF Fitting. *J. Synchrotron Radiat.* **2001**, *8*, 322–324.
28. Rehr, J. J.; Albers, R. C. Theoretical Approaches to X-Ray Absorption Fine Structure. *Rev. Mod. Phys.* **2000**, *72*, 621–654.
29. Ravel, B.; Newville, M. Athena, Artemis, Hephaestus: Data Analysis for X-Ray Absorption Spectroscopy Using Ifeffit. *J. Synchrotron Radiat.* **2005**, *12*, 537–541.S.